Framework Service Contract EEA/DIS/R0/20/001 Lot 1 for Services supporting the European Environment Agency's (EEA) cross-cutting coordination of the Copernicus programme's in situ data activities – Observational data

ASSESSING POTENTIAL OF EMERGING OBSERVATIONS FOR COPERNICUS ARCTIC SERVICE

Jun She, Vilnis Frishfelds and Ole Krarup Leth
Danish Meteorological Institute

Issue: 2.0
Date: 09/09/2021

[DOCUMENT RELEASE]

	Name(s)	**Affiliation**
Coordinated by:	Erik Buch	EuroGOOS
Contributions:	Jun She, Vilnis Frishfelds and Ole Krarup Leth	Danish Meteorological Institute
Approval:		
Prepared for:	European Environment Agency (EEA)	
Represented by: (Project Manager)	Henrik Steen Andersen	
Contract No.	EEA/DIS/R0/20/001 Lot 1	

[Change Record]

Version	**Date**	**Changes**
1.0	15 April 2021	Version 1
2.0	09 September 2021	Version 2 – updated after CMEMS review

Glossary

ARC MFC	Arctic Monitoring and Forecasting Centre
BDC	Berring Data Collective
CMEMS	Copernicus Marine Environmental Monitoring Service
cRMSE	Centred root mean square error
CTD	Conductivity, temperature, and depth
CTD-SRDL	CTD-satellite relay data logger
EMODnet	The European Marine Observation and Data Network
ERDDAP	Environmental Research Division's Data Access Program
GPS	Global Position System
GSR	Greenland-Scotland Ridge
ICES	International Council for the Exploration of the Sea
MEOP	Marine Mammals Exploring the Oceans Pole to Pole
MFC	Monitoring and Forecasting Centre
MIZ	Marginal Ice Zone
NRT	Near Real Time
QUID	QUality IDentification report
RMSD	Root mean square deviation
RMSE	Root mean square error
SeaDataNet	Pan-European infrastructure for ocean & marine data management.
SP2T	Pressure and temperature
STPS	Pressure, temperature and conductivity)
T/S	Temperature and Salinity
TOPAZ	Operational Prediction system for the North Atlantic European coastal Zones
UDASH	Unified Database for Arctic and Subarctic Hydrography
WOD	World Ocean Database

Executive Summary

This is an analysis of the usability of temperature and salinity measurements obtained from instruments mounted on fishing gear and on marine mammals for ocean model validation. The fishing gear observations have several characteristics, i.e., they are operational, accessible in near real-time, high spatial resolution and covering mainly coastal and offshore waters. The marine mammal observations are also operational, have high spatial and temporal resolution and covering pan-Arctic waters, especially marginal ice zone, coastal and offshore waters, and provide also quite good temporal coverage in winter months. These features are complementary with traditional research vessel observations, which are of low frequency and mainly covering the summer months and open waters.

In this report the observed water temperature and salinity data from fishing gears and marine mammals are compared with the ARC MFC analysis and 12hour forecast data and CMEMS global reanalysis product, respectively. No quality problems are found in the observations. The validation results show that the fishing gear and marine mammal observations are valuable and unique for identifying model error features in the Arctic coastal and marginal seas, providing hints for further model improvements. In general, it can be concluded that the instruments used for oceanographic observations from fishing gears and the animal borne instruments are of documented and satisfactory quality to be used for modelling purposes.

In the Baffin Bay, the inter-comparison of model hydrography with hydrography obtained based on observations from fishing gear shows that the model has shallower mixing layer in summer and sometimes stronger mixing in the winter. In the coastal waters, observed lower salinity in the surface layer is missing in the model. In general ARC MFC water temperature forecast is ~0.5°C colder than the observations. In November 2019 the ARC MFC model ocean is found to be 1-2°C warmer in 200-300 m depth in open waters around Faroe Islands. The observations in Norwegian coastal waters show that the model fails to simulate the vertical structure of four water mass layers in November 2020.

Temperature and salinity profile measurements from marine mammals are used to validate CMEMS global daily reanalysis products. The results show that the global reanalysis has significant errors in marginal ice zone with low ice concentration, with temperature bias more than 5 °C and surface salinity bias more than 2 psu, much larger than what is observed in other ocean areas with the same model. This is probably related to the modelling error on the sea ice. In the vertical direction the model temperature bias and centred root mean square error (cRMSE) are approximately constant in the upper 50 m with values of 0.18 °C and 1.16 °C, respectively. The model error increases with depth and reaches maximum values in 100-150 m depth, where the thermocline is located, with bias of 0.48°C and cRMSE of 1.57°C. For salinity, the model ocean is saltier than the observations in all vertical depths, with the largest error at the surface (0.50 psu for bias and 1.42 psu for cRMSE), decreasing with depth and reaching minimum in 600-700 m water depth (0.04psu for bias and 0.08psu for cRMSE).

1 Introduction

For Copernicus Marine Environmental Monitoring Service (CMEMS modelling of the Arctic Ocean, an estimation of observation adequacy suggests that 200 Temperature and Salinity (T/S) profiles per day are required by the ARC MFC (LeTraon et al., 2019, Buch et al., 2019) for data assimilation, validation and other purposes. The first Arctic Data Report (Buch et al., 2019) shows, however, that there are only about 23 profiles available in average during the period from 1980 to 2015 in the integrated UDASH database. In recent years, the number of observations has increased. The number of T/S profiles per annum from SeaDataNet, ICES, EMODnet and WOD can reach 18008-19877 in total for the period 2016-2018, i.e., 49-56 profiles per day. The conclusion is that current T/S data availability in the Arctic Ocean is still far from sufficient to adequately support the ARC MFC.

Using fishing vessels to make T/S observations in the Arctic marginal seas is a cost-effective way of monitoring, and the method has a big potential to fill the current data gaps especially in the Arctic coastal seas. In the last couple of years, T/S profiles have also become available from fishing vessels in the Arctic, although the amount of data is still quite small. Another cost-effective monitoring in the Arctic is to use animal-borne sensors, which has produced huge amount of data in recent years. Neither the fishing vessel data nor data from marine mammal borne instruments have been used in CMEMS ARC MFC and European operational ocean forecast. It is important to investigate if these data have suitable quality and potential for being used by CMEMS. In this report a preliminary quality feasibility assessment of the existing data from fishing vessels and marine mammal borne instruments will be performed by applying the available data sets to validate the CMEMS ARC MFC and Global MFC model results.

2 Review of existing observation technology and data quality

2.1 Fishing vessel data: sensors and quality

The gear used to catch fish is often set out close to the sea floor and then hauled back up, offering a potential platform for sensors to measure basic oceanographic parameters while fishermen are performing their normal fishing operations. Fishing vessels are able to almost continuously collect a large amount of data on a large spatial scale, thus fostering fishery- and oceanographic research at a much lower cost than those incurred from using dedicated oceanographic vessels (Patti et al., 2016).

The popular NKE sensors represent a better option nowadays due to their characteristics, including a fast response time (0.5 s) and high accuracy (temperature ± 0.05°C and pressure 0.3% of full scale for NKE) (Patti et al., 2016; Martinelli et al. 2016). Hence, the use of the NKE sensors allows the collection of reliable temperature profiles during the descent phase of the fishing gear (Martinelli et al., 2016).

The sensors used to collect the data showcased below are NKE WiSens CTD and TD (https://nke-instrumentation.com/produit/wisens-ctd/), and Zebra Tech Moana TD (https://www.zebra-tech.co.nz/moana/). Both of these sensors have rapid measurement response time, which is necessary to measure accurate water column profiles during the relatively rapid ascent and descent of fishing gears (Martinelli et al., 2016). The manufacturer specified temperature accuracy for the NKE and Moana sensors is ± 0.005°C and ± 0.05°C, respectively.

Both the NKE and Moana probes are designed specifically to be mounted on fishing gear and provide robust and reliable measurements under these conditions. Additional special nylon cases have been built for the sensors in order to protect them and to allow them to be fixed to fishing gear. In addition, once out of the water these probes can automatically send the collected data wireless to a vessel hub unit which also allows for constant GPS geolocation. From this hub, the data can then be relayed onto an endpoint using a cellular, or the vessel's satellite, communication system without power or antenna size constraints. The availability of NRT data sets may be of great importance for oceanographic models and forecasting purposes.

2.2 Marine mammal observations

Marine mammals equipped with bio-logging devices have been used to fill the data gaps in Arctic and Antarctic Oceans where logistically difficult to make observations. The effort is coordinated by the scientific community through the MEOP (Marine Mammals Exploring the Oceans Pole to Pole, http://meop.net) which is a consortium of international researchers dedicated to sharing animal-derived data and knowledge about the polar oceans (Treasure et

al., 2017). Following information of the sensors and quality control procedure was described in Treasure et al., 2017.

The sensor used in most of the MEOP data collection is the CTD-satellite relay data logger (CTD-SRDL), which is an autonomous tag that records location together with vertical profiles of conductivity, temperature, and pressure to a maximum depth of ~2,000 m, depending on the species involved (Boehme et al., 2009; Photopoulou et al., 2015). Vertical profiles of temperature, salinity and density can be inferred from this information. A post-processing procedure is applied to oceanographic data to ensure the best possible data quality (Roquet et al., 2014). New CTD-SRDLs include enhanced data collection capabilities.

The CTD-SRDLs are built at the Sea Mammal Research Unit at the University of St Andrews (UK), incorporating the miniaturized CTD unit manufactured by Valeport Ltd. (Devon, UK). The sensor head consists of a pressure transducer, a platinum resistance thermometer, and an inductive cell for measuring conductivity. The temperature and conductivity sensors have a precision (repeatability) of 0.005°C and 0.005 mS cm–1, respectively. Before being taken into the field, devices are calibrated in the laboratory.

CTD-SRDLs record oceanographic profiles during the ascent of the animals (Boehme et al., 2009; Roquet et al., 2011; Photopoulou et al., 2015) at a 1 Hz sampling frequency, retaining only the deepest dive in each six-hour time interval. Profiles are then telemetered in a compressed form (between 10 and 25 data points per profile, depending on the tag program) through the Advanced Research and Global Observation Satellite (ARGOS) system. Geolocation is determined by satellite triangulation with a typical accuracy of a few kilometers. The transmission occurs up to four times per day.

The MEOP data portal distributes data mainly from CTD-SRDL tags because it is currently the only available tag that incorporates both temperature and salinity measurements with an accuracy suitable for oceanographic studies (~0.02°C for temperature, ~0.03 psu for salinity). A secondary database (the MEOP-TDR database) has recently been released that incorporates temperature profiles using the popular MK9/MK10 Wildlife Computers tags with lower accuracy (~0.5°C) but higher spatial resolution (~60 profiles/day).

New sensor capabilities are also being added. The Cyclops 7 fluorometer is a compact cylinder (110 mm × 25 mm after removal of the end cap), low-energy-consumption, single-channel fluorescence detector that can be integrated into the CTD-SRDL tag (Guinet et al., 2013). It has been attached to elephant seal tags deployed in the Indian sector of the Southern Ocean since 2007, yielding a unique data set of in situ chlorophyll measurements in this extremely data poor, highly productive region. Also, an oxygen sensor has been successfully incorporated into a few CTD-SRDLs (Bailleul et al., 2015). While this technology is still in early development, it

has great potential for the future of integrated biophysical and biogeochemical research, as oxygen provides a fundamental link between physical and biogeochemical processes.

In general it can be concluded that the instruments used for oceanographic observations from fishing vessels and animal borne instruments are of documented and satisfactory quality to be used for model assimilation and validation. It is therefore in the following model validation exercise assumed that the available observations represent the true ocean state and can be used to evaluate the quality of the model forecasts.

3 Input data and methodology

3.1 Observations

Fishing vessel data: coastal and shelf seas in the Arctic are among the least monitored areas of the world ocean yet fished both by commercial vessels and indigenous fishers. Berring Data Collective (BDC) has deployed oceanographic sensors on the fishing gears of several fishing vessels in the Arctic (60-90°N) since 2019. The data are available in the EMODnet Physics Data portal, the BDC ERDDAP server, and recently via CMEMS IN SITU TAC.

There are presently 6 fishing vessels collecting data in the Arctic in which all of them measure temperature but only one vessel measures salinity. The monitoring areas are Nordic Seas and West Greenland waters (Fig. 1). Only observation data that are above 60° N latitude are included in this analysis.

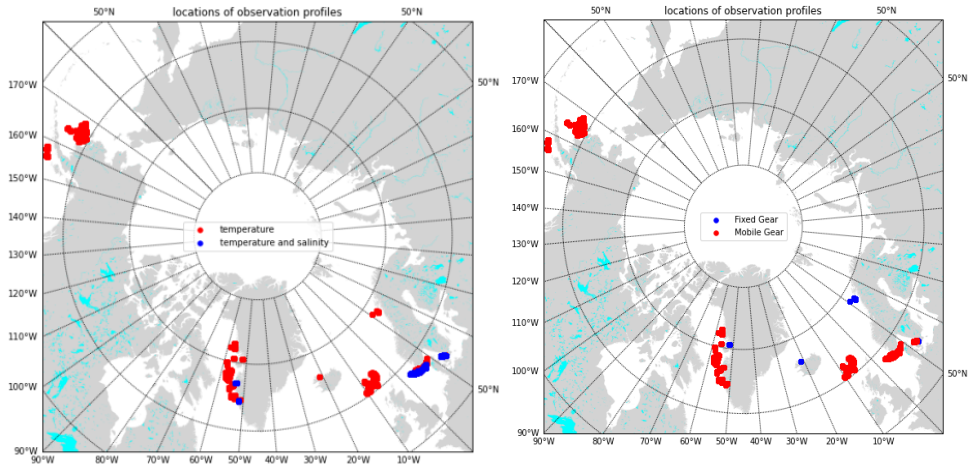

Figure 1. Locations of fishing vessel observations in the Arctic seas. Left figure: red – mobile gear; blue – fixed gear; right figure: red – water temperature profiles only; blue – both water temperature and salinity profiles are available.

Marine mammal observations: The marine mammal tagged T/S profile data are available from EMODnet Physics ERDDAP server, including MEOP data from 2004-2014 (Fig. 2). The ERDDAP (https://erddap.emodnet-physics.eu/erddap/index.html) is a data server that gives users a simple, consistent way to download subsets of scientific datasets in common file formats and make graphs and maps. These data are also available in CMEMS INS-TAC and MEOP data portal

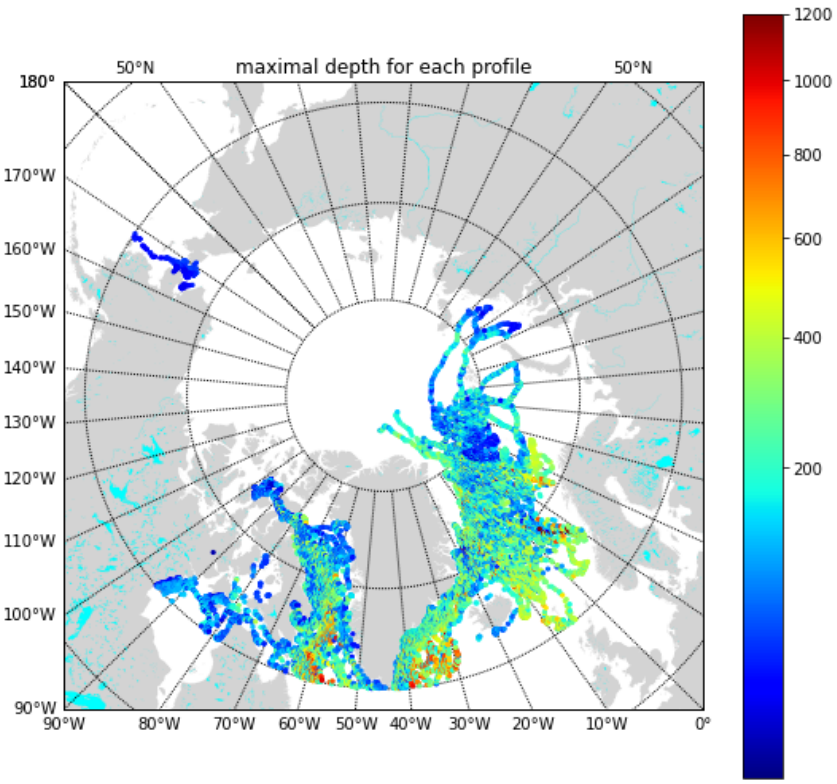

Figure 2. Geographic distribution of T/S profile monitoring stations from the MEOP database for during the 2004-2014 period.

3.2 Model data

Model data are downloaded from CMEMS website. For the fishing vessel inter-comparison study, an analysis and 12h forecast product generated by ARC MFC using TOPAZ4 Arctic Ocean Forecasting System is used (Fig. 3, left). The model product covers the entire Arctic with 12.5 km horizontal resolution and has 25 vertical layers, including daily 3D temperature and salinity fields and hourly surface temperature and salinity fields (Fig. 3, left). A detailed description of the product can be found in
https://resources.marine.copernicus.eu/documents/PUM/CMEMS-ARC-PUM-002-ALL.pdf
and a quality identification report (QUID) can be found in
https://resources.marine.copernicus.eu/documents/QUID/CMEMS-ARC-QUID-002-001a.pdf

For inter-comparison with Marine mammal observations, CMEMS Global MFC reanalysis data are used (product ID: GLOBAL_REANALYSIS_PHY_001_030, Fig. 3, right). This is because the ARC MFC reanalysis only provide monthly averages for three-dimensional temperature and salinity fields, while the GLO MFC provides daily data which covers entire Arctic Ocean with 1/12 degree horizontal resolution and 50 vertical layers (Fig. 3b). A detailed description of the product can be found in http://marine.copernicus.eu/documents/PUM/CMEMS-GLO-PUM-001-030.pdf and a quality identification report (QUID) can be found in http://marine.copernicus.eu/documents/QUID/CMEMS-GLO-QUID-001-030.pdf.

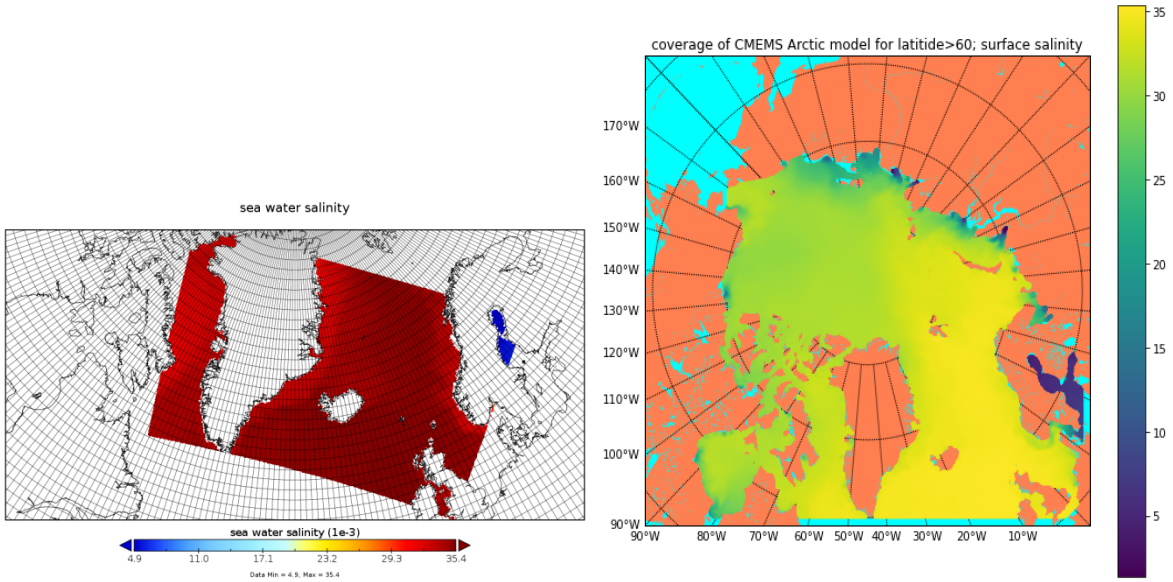

Figure 3. Geographic areas of model data used for fishing vessel observation study (left) and marine mammal tagged observation study (right)

3.3 Validation method

For inter-comparing model data and fishing vessel observations, due to the limited amount of data, only qualitative comparison was made. For the marine mammal observations, quantitative validation of the CMEMS global reanalysis was carried out in terms of model error distribution in vertical, horizontal and temporal dimensions. Simple error statistics, bias and centred root mean square error (cRMSE) or centred root mean square deviation (cRMSD) were applied.

Suppose we have the discrete observation data *r(i,k,t)* defined in time and space and we need to verify the model product data *p (i,k,t)* against the reference data. The *(i,k,t)* denote space (horizontal and vertical) and time indices, respectively. The error statistics used in this report is thus defined as follows:

$$\mathrm{bias}(p,r) = \mathrm{mean}(p) - \mathrm{mean}(r) \quad (1)$$

$$\mathrm{cRMSD}(p,r) = cRMSE(p,r) = \sqrt{\frac{1}{N_i}\frac{1}{N_k}\frac{1}{N_t}\sum_{i=1}^{N_i}\sum_{k=1}^{N_k}\sum_{t=1}^{N_t}\Big(\big(p-\mathrm{mean}(p)\big)-\big(r-\mathrm{mean}(r)\big)\Big)^2} \quad (2)$$

N_t is the total number of time steps covered, the N_i, N_k are the total number of horizontal and vertical observation indexes.

4 Result analysis

4.1 Feasibility assessment of fishing vessel observations for CMEMS

The feasibility of fishing vessel data for scientific use has been partly documented in Van Vranken et al. (2020). In this study we are going to test the feasibility of using fishing vessel observed T/S data to validate the CMEMS Arctic forecast products. This is done vessel by vessel.

Vessel 2: this trawl vessel takes observations in coastal waters in Baffin Bay (Fig. 4a, left). The observation period is June 2019 – Jan. 2020. An upper layer warming is found from July to October 2019, followed by autumn and winter period with cooling and enhanced mixing (Fig. 4a, up-right). In the summer the model has shallower mixed layer leading to significant negative bias at the bottom of the mixing layer (around 20 m depth, Fig. 4b). The intermediate cold layer is well simulated. In December 2019, the model has a too strong mixing (Fig. 4a lower right panel) associated with negative bias below 50 m water depth (Fig. 4b). The shallower mixing in summer / deeper mixing in winter is a known issue and probably a more general issue of ocean models (Ali et al., 2019).

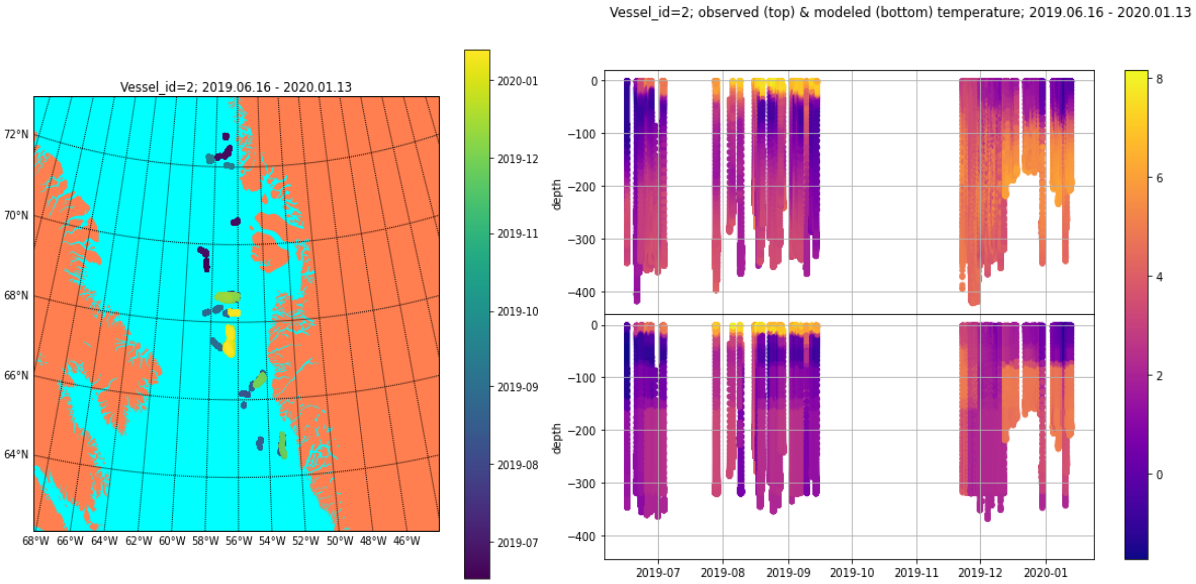

Figure 4a. Vessel 2 locations and timing (left, shown in different colors); observed (upper right panel) and modelled (lower right panel) water temperature

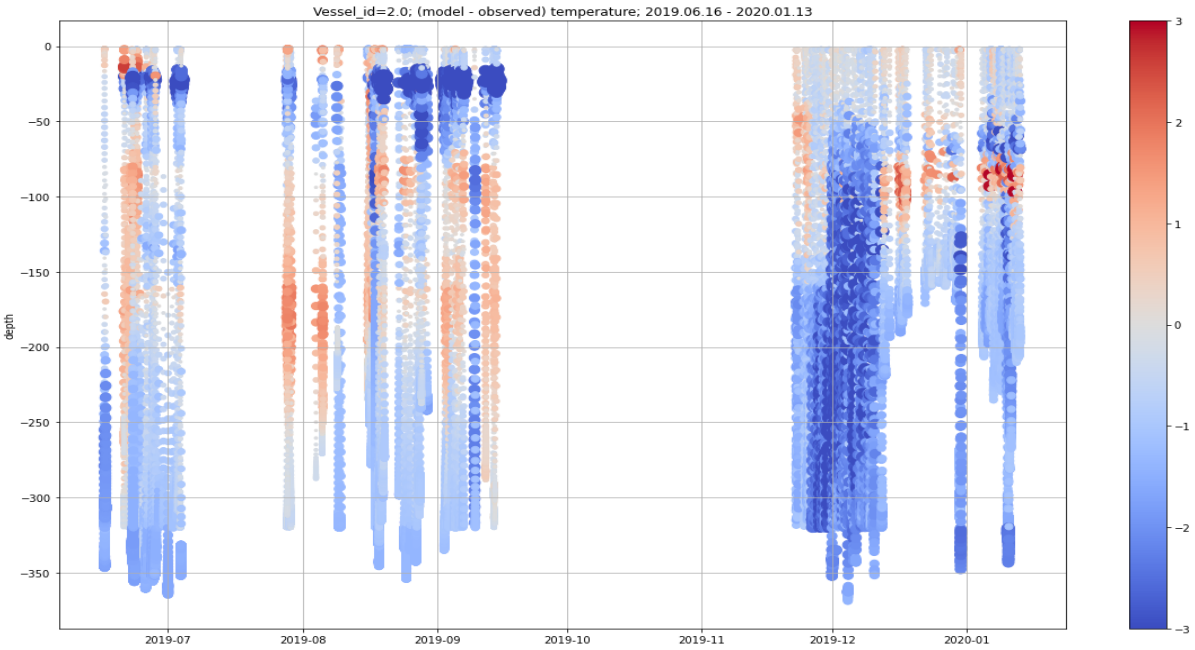

Figure 4b. Differences between the observed and modelled water temperature (Vessel2)

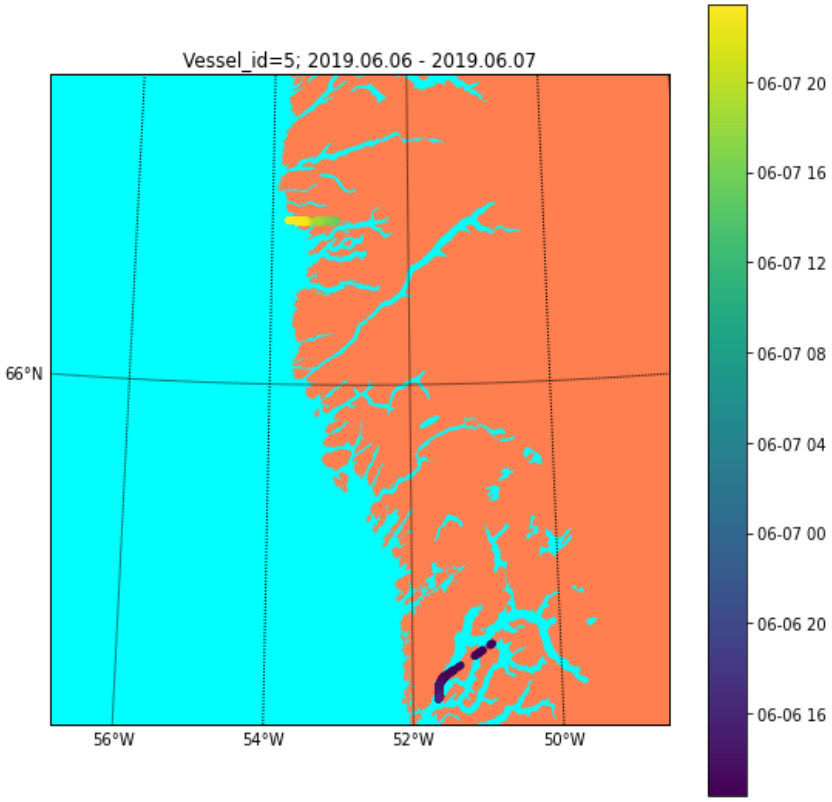

Figure 5a: Vessel 5 locations and timing (shown in different colors);

Vessel 5: this trawl vessel took observations in Fjord waters in Baffin Bay in a two-day period in June 2019 (Fig. 5a). Parts of the fjords is not resolved in the model product (Fig. 3, left), so the model data is missing for parts of the observed locations (Fig. 5b). Temperature is stratified with warmer water in the upper 5-10 meters and with colder water below. In the mixed layer,

the model water is a couple of degree colder than the observations thus less stratified (Fig. 5b left). For the salinity, water in the upper 5-10 meter is 1-2 psu fresher than the lower layer waters. However, this feature is not captured by the model. Furthermore, salinity observations display lower salinities in the entire water column than the model.

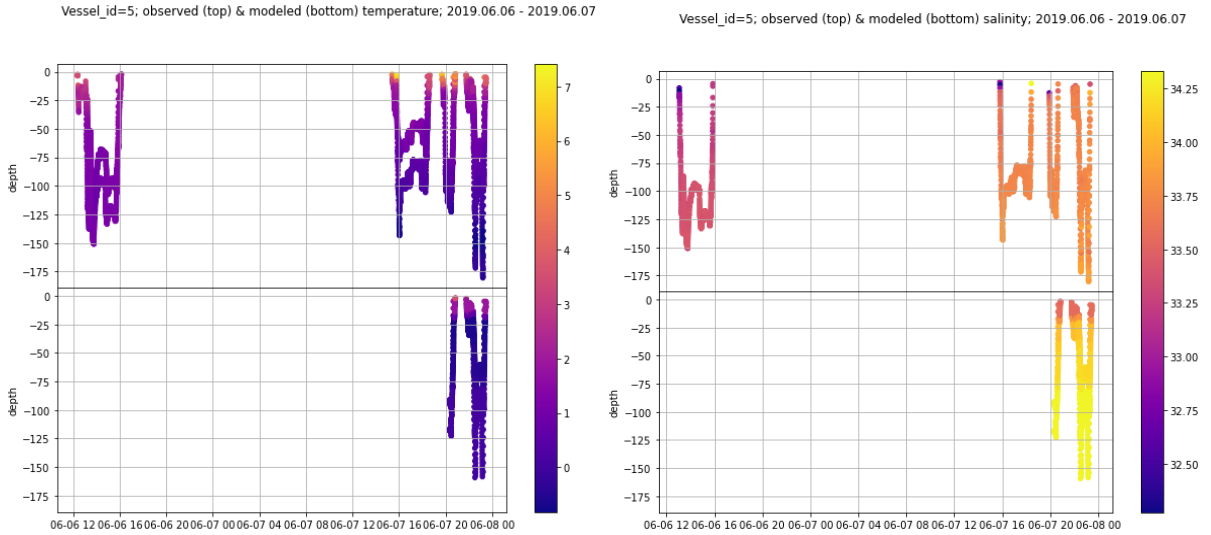

Figure 5b. Observed (upper panel) and modelled (lower panel) water temperature (left) and salinity (Vessel 5). Note that there are two values at two different depths for the same time which is because that there are two sensors in different depths

Vessel 6: this longline fishing vessel took water temperature observations in Icelandic coastal waters between 04-12 GMT, 16 May 2019 (Fig. 6a), including a descending profile, a period with bottom measurements and then an ascending profile. The descending profile at 04GMT shows well-mixed water column with water temperature between 5.2-5.4^{o}C with slightly increasing temperature from 20 m depth to the bottom. The bottom temperature becomes a bit colder to 5^{o}C at 11:30 GMT. Afterwards the ascending profile also shows a well-mixed water column (Fig. 6a). The model results show a stronger stratification with about 1^{o}C warmer in the upper layer and -1^{o}C colder at the bottom layer (Fig. 6b).

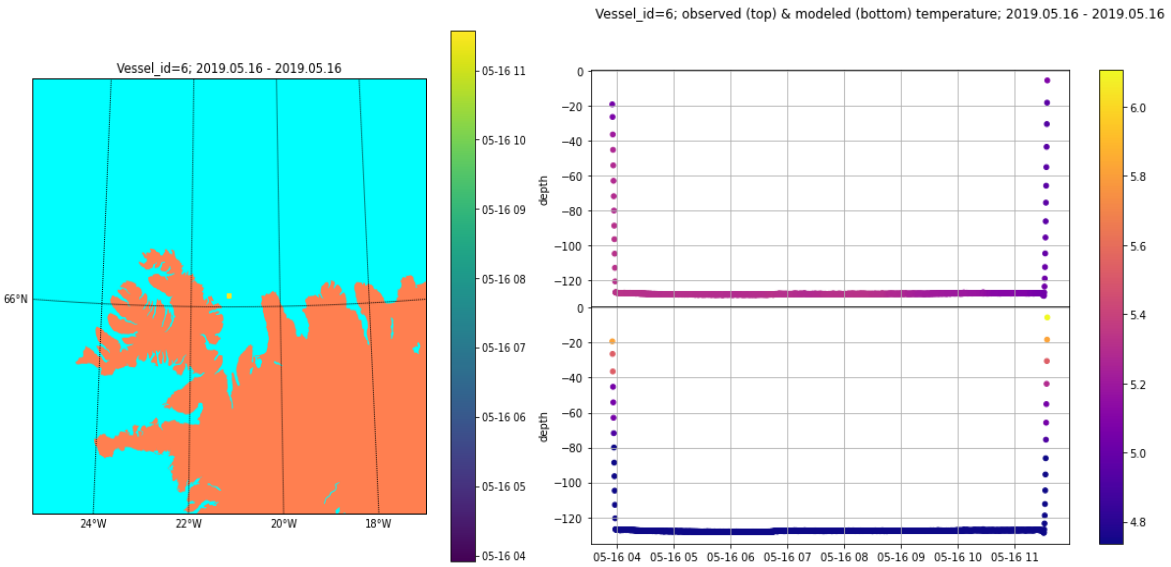

Figure 6a. Vessel 6 (Fixed Gear) locations and timing (left, shown in different colors); observed (upper right panel) and modelled (lower right panel) water temperature

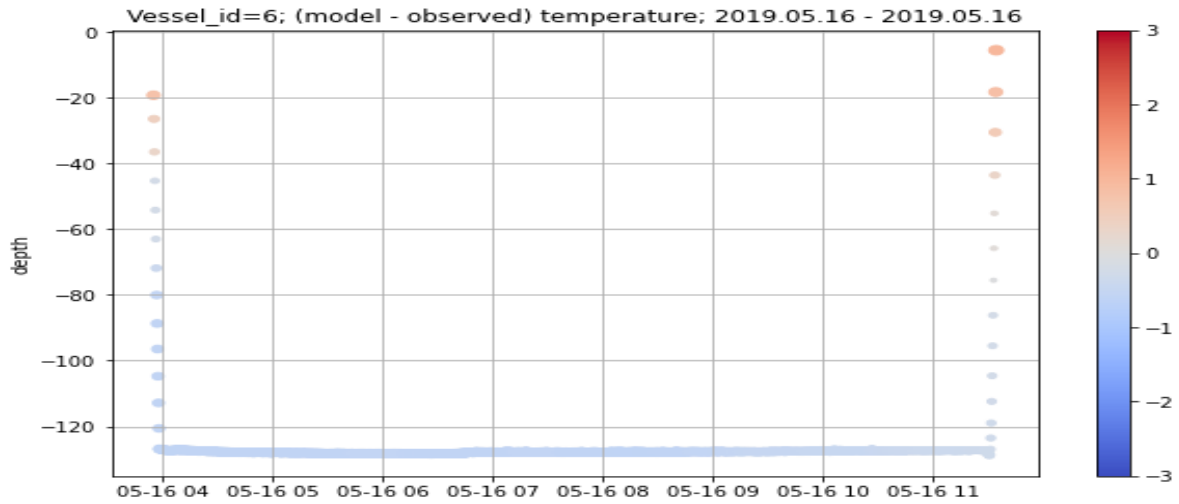

Figure 6b. Differences between the observed and modelled water temperature (Vessel 6)

Vessel 14: this trawl vessel took temperature observations in the water column down to 350 m depth in Faroe Island waters during 8 Nov. – 2 Dec. 2019 (Fig. 7a, left). It started from offshore waters west of the Faroe Islands and then moved clockwise around the islands. Both observations and the model show a well-mixed ocean area (Fig. 7a, right). One distinguishing feature is that the model ocean is warmer than the observations by up to 3°C in 200-300 m water layers. (Fig. 7b).

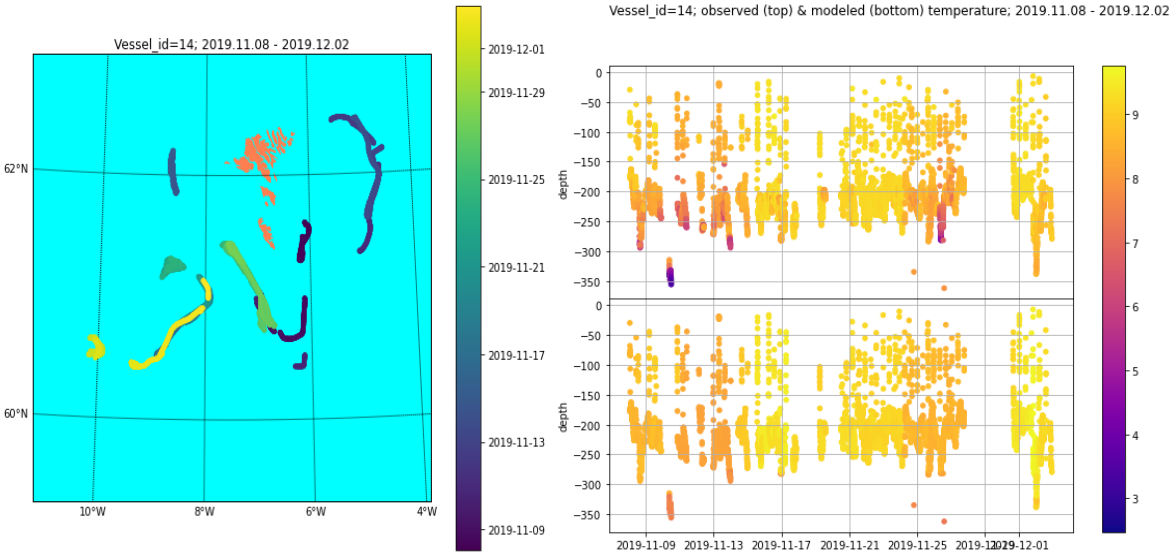

Figure 7a. Vessel 14 locations and timing (left, shown in different colours); observed (upper right panel) and modelled (lower right panel) water temperature

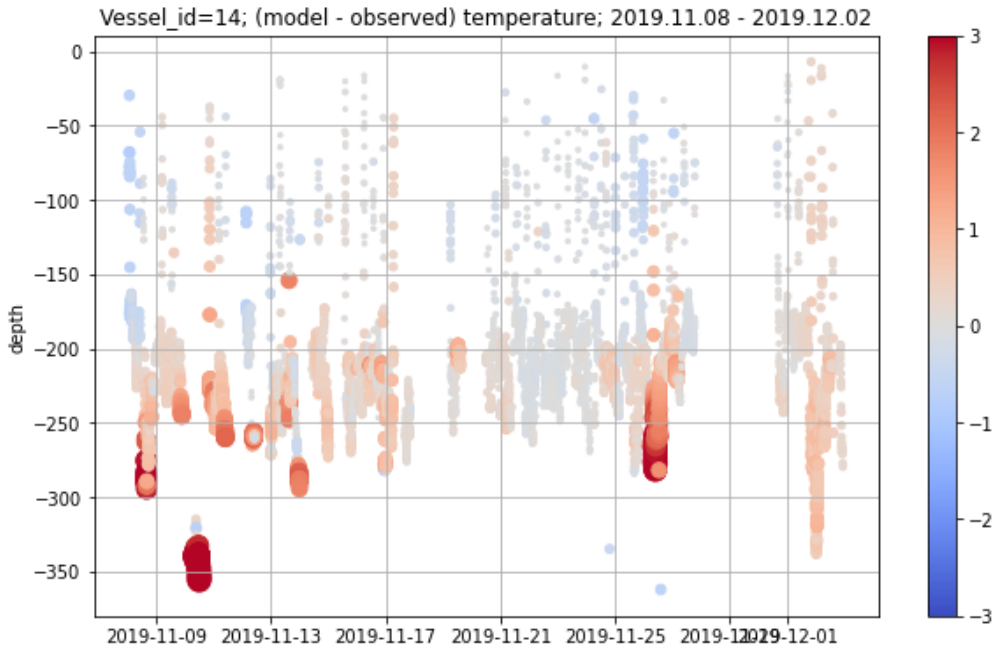

Figure 7b. Differences between the observed and modelled water temperature (Vessel 14)

Vessel 63: the vessel took temperature observations in the water column down to 650 m depth at three locations in Norwegian coastal and offshore waters during 10 Aug. – 26 Nov. 2020 (Fig. 8, left). Observation and model data show a good agreement with shallow mixing layer in August and well mixed waters in November (Fig. 8 right). The deeper observation at the shelf edge is with a sensor deployed using bottom longline gear, and the shallower observations using a bottom net call a Danish-seine.

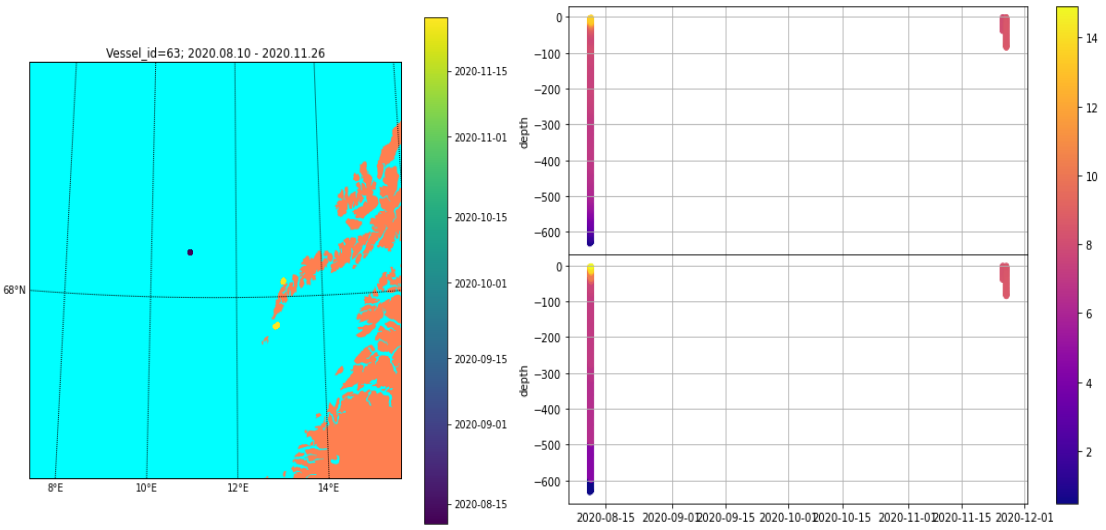

Figure 8. Vessel 63 sampling locations and timing (left, shown in different colours); observed (upper right panel) and modelled (lower right panel) water temperature

Vessel 68: the vessel took temperature observations in the water column down to 1200 m depth at three locations in Uummannaq Fjord, West Greenland during 3 – 9 Nov. 2020 (Fig. 9a, left). These observations are from indigenous Inuit fishers in collaboration with Uummannaq Polar Institute. Observations show four layers of water masses: the upper (50 m) cold water, a warmer layer between 50-100 m depth, a cold-water layer between 100-300 m depth and a warm layer below 300 m (Fig. 8a right). The model ocean only shows a two-layer water mass distribution, i.e., a cold-water layer in the upper 180 m and a warmer layer below 180 m (Fig. 9, right). It is noted that the model bathymetry only reaches 600 m while the observations measured in almost 1200 m. This local deep bathymetry was also recorded in multibeam echo sounding surveys (Rignot et al., 2016).

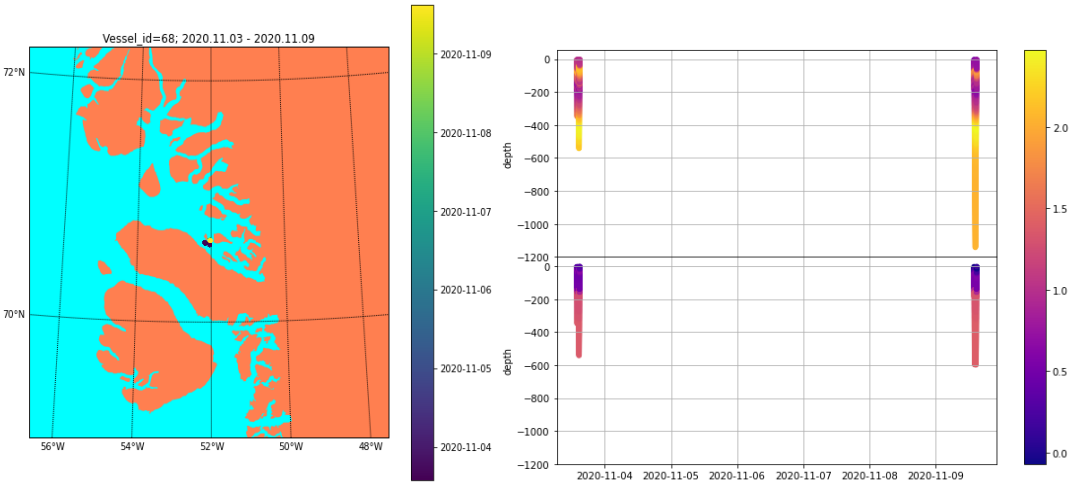

Figure 9. Vessel 68 sampling locations and timing (left, shown in different colors); observed (upper right panel) and modelled (lower right panel) water temperature

Error statistics of the ARC MFC forecast product is shown in Table 1. The model water temperature forecast is colder than the observations, with bias from -1.0 ~ 0.3 °C and cRMSE between 0.1 ~0.8°C. Only one fishing gear in Faroe Island waters has salinity data. The salinity forecast has a positive bias of 0.4 psu. It should be noted the resolution of ARC-MFC product used in the study of 12.5 Km,

therefore results of vessels 5 and 68 which samples in near shore and fjords are less representative than other vessels.

Table 1. Error statistics of ARC MFC water temperature (T) and salinity (S) forecast validated against fishing gear observations at the model layers. T_count and S_count is number of observations for temperature and salinity, respectively.

Vessel id	Mean latitude (°N)	Mean longitude (°E)	T_cRMSE [K]	T_bias [K] (model-obs.)	T_count	S_cRMSE [PSU]	S_bias [PSU] (model-obs.)	S_count
2	68.223	-56.146	0,71	-0,84	68042	NaN	NaN	0
5	65.920	-52.716	0,78	-1,04	1028	0.21	0.45	477
6	66.090	-21.146	0,10	-0,52	1835	NaN	NaN	0
14	61.165	-7.502	0,53	0,29	6402	NaN	NaN	0
63	68.214	11.510	0,51	-0,26	491	NaN	NaN	0
68	70.663	-52.064	0,62	-0,55	845	NaN	NaN	0

4.2 Feasibility assessment of Marine mammal observations for CMEMS

In this section, results of model-observation inter-comparison are presented in both spatial and temporal dimensions.

4.2.1 General model-observation inter-comparison

Vertical features: the error distribution of the global reanalysis water temperature and salinity with water depth are displayed in Fig. 10. The bias and cRMSE show similar vertical distribution (Fig. 10). For water temperature, the model gives higher values than the observations. The model data bias and cRMSE are fairly constant in the upper 50 m with values of about 0.18°C and 1.16°C, respectively. Both bias and cRMSE increase with depth to reach maximum values at the depth of the thermocline (100-150 m depth) of 0.48°C and 1.57°C, respectively. From there the bias and cRMSE decrease with water depth. It is evident from the figure that the amount of data decreases sharply at the depth of the thermocline. This indicates that the sea lions normally do not stay at depth below the thermocline for long periods of time. For salinity, the model ocean is saltier than the observations in all vertical layers, with the largest error at the surface (0.50 psu for bias and 1.42 psu for cRMSE), decreasing with depth and reaching a minimum in 600-700 m water depth (0.04psu for bias and 0.08psu for cRMSE). The errors increase slightly at depths below 700 m (Fig. 10).

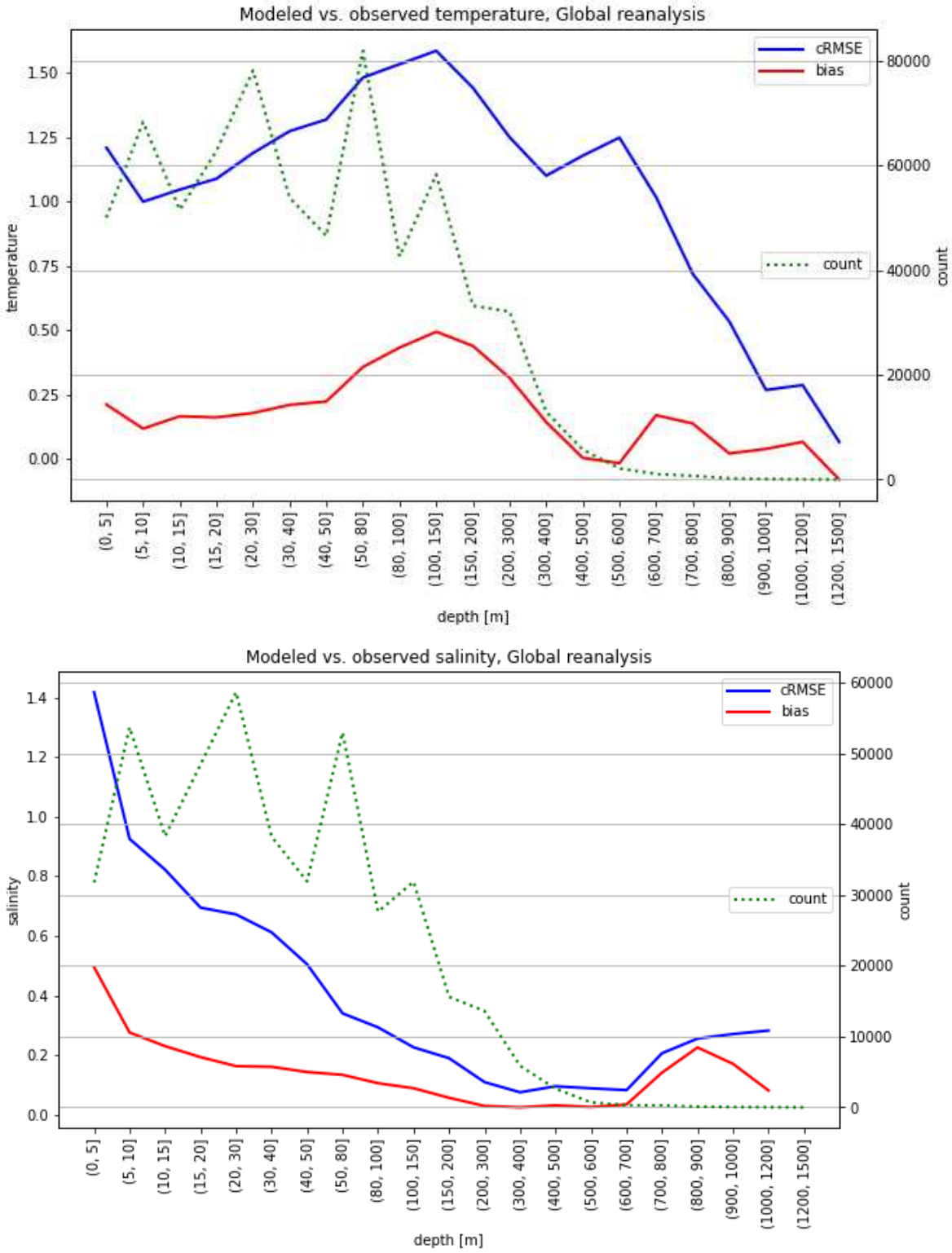

Figure 10. Error distribution of CMEMS global reanalysis product with the water depth against marine mammal observations for water temperature (upper panel) and salinity (lower panel): Red-bias, blue-cRMSE and green-number of observations. The x-axis is the depth interval, left y-axis indicates the error level while the right y-axis shows the number of observations.

Horizontal features: Fig. 11 shows the geographic distribution of the model errors for temperature and salinity in the upper 10 m of the water column. For water temperature, the

model has for most of the sampling stations a positive bias within 1°C. Large bias up to and above 5 °C is found in the southern Greenland Marginal Ice Zone (MIZ, Fig. 11, upper-left), which is probably related to uncertainties in modelling coastal sea ice in this region by the CMEMS global ocean model. High cRMSE >1.5°C are also mainly associated with MIZs (Fig. 11, upper-right). For salinity, areas with negative bias are found mainly north of 80°N. The negative signal also spreads to the south along the ice edge. Another area with negative salinity bias is in southern Baffin Bay. The remaining area has positive salinity bias with its largest value in SE Greenland coastal waters and northern part of the Kara Sea (Fig. 11, lower-left). Large salinity cRMSE (>1 psu) mainly occurs in MIZ in off East Greenland (Fig. 11, lower-right).

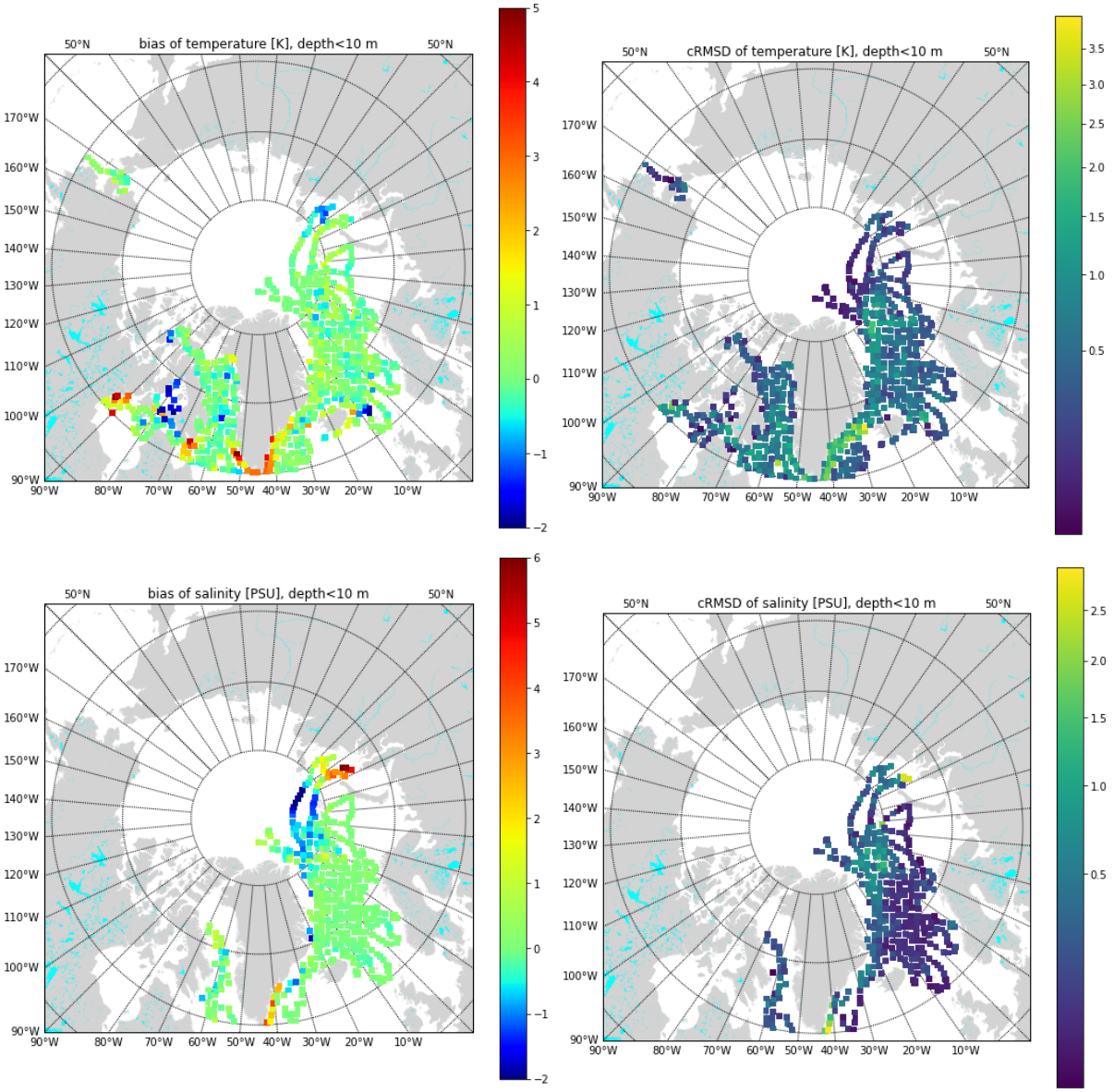

Figure 11. Horizontal error distribution of water temperature (upper panel) and salinity (lower panel) in the upper 10 meters of the CMEMS global reanalysis products compared to observations obtained from marine mammals.

Seasonal variability: monthly averages of the model bias and cRMSE are displayed in Fig. 12. Major feature is the error maxima in July and August, both in the bias and cRMSE for temperature and salinity. Noticing the minimum sampling number in July, the July error statistics may be affected by the uneven sampling.

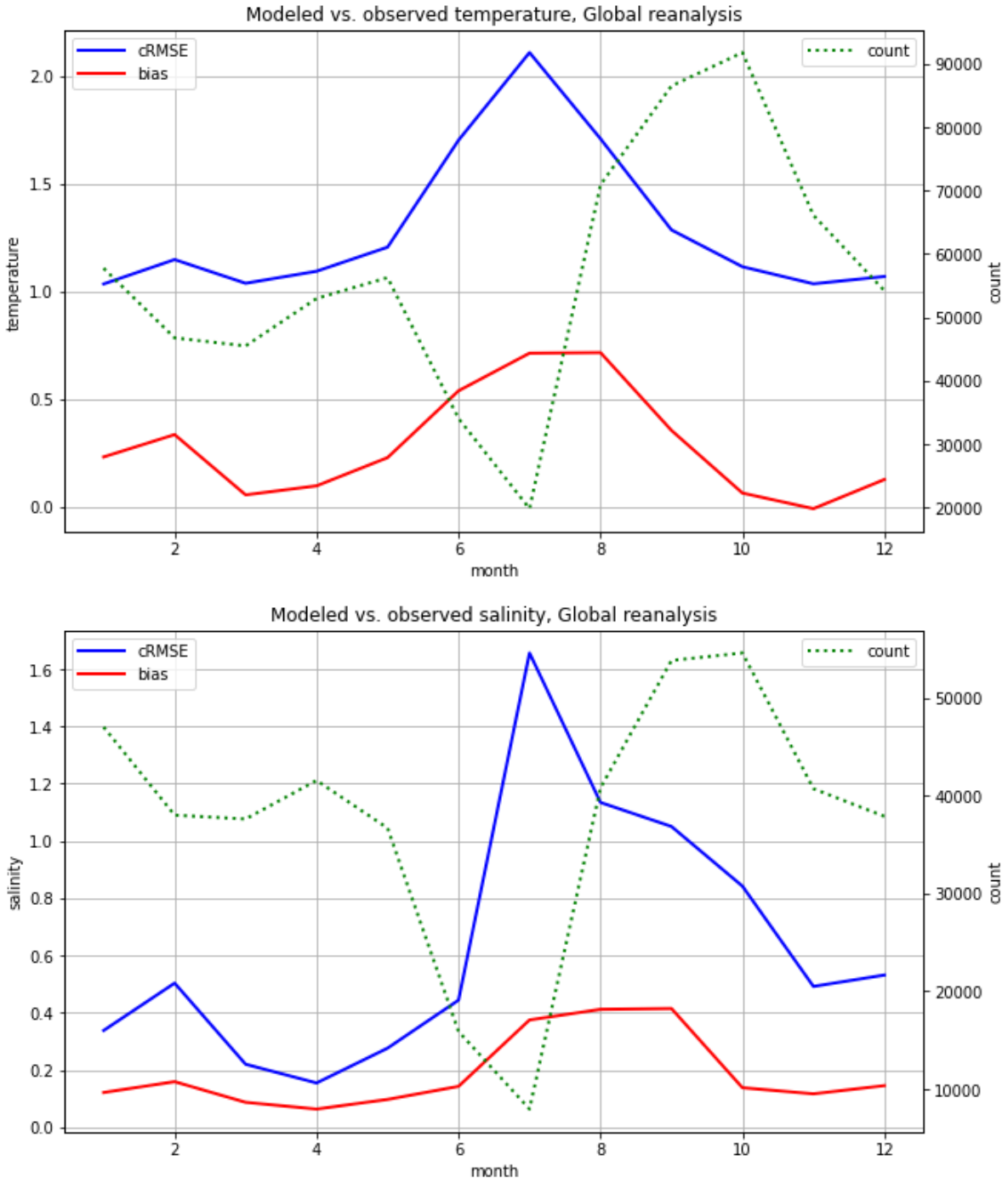

Figure 12. Similar as Fig. 10 but for error distribution with months.

4.2.2 Stations with large model-observation anomalies

There are some stations which have large anomalies when comparing the model data with observations. Figure 13 displays station locations with large model-observation differences,

i.e., absolute temperature bias >5ºC and salinity bias >2 psu. In southern Greenlandic waters and Svalbard coastal waters, the anomalous model results are mainly associated with MIZ, indicating that the model probably also has relatively large errors in modelling the sea ice. The model also shows large salinity error in the northern part of the Kara Sea. For both models and observations, the spatial patterns of salinity are similar which show minimum salinity in the north of Kara Sea.

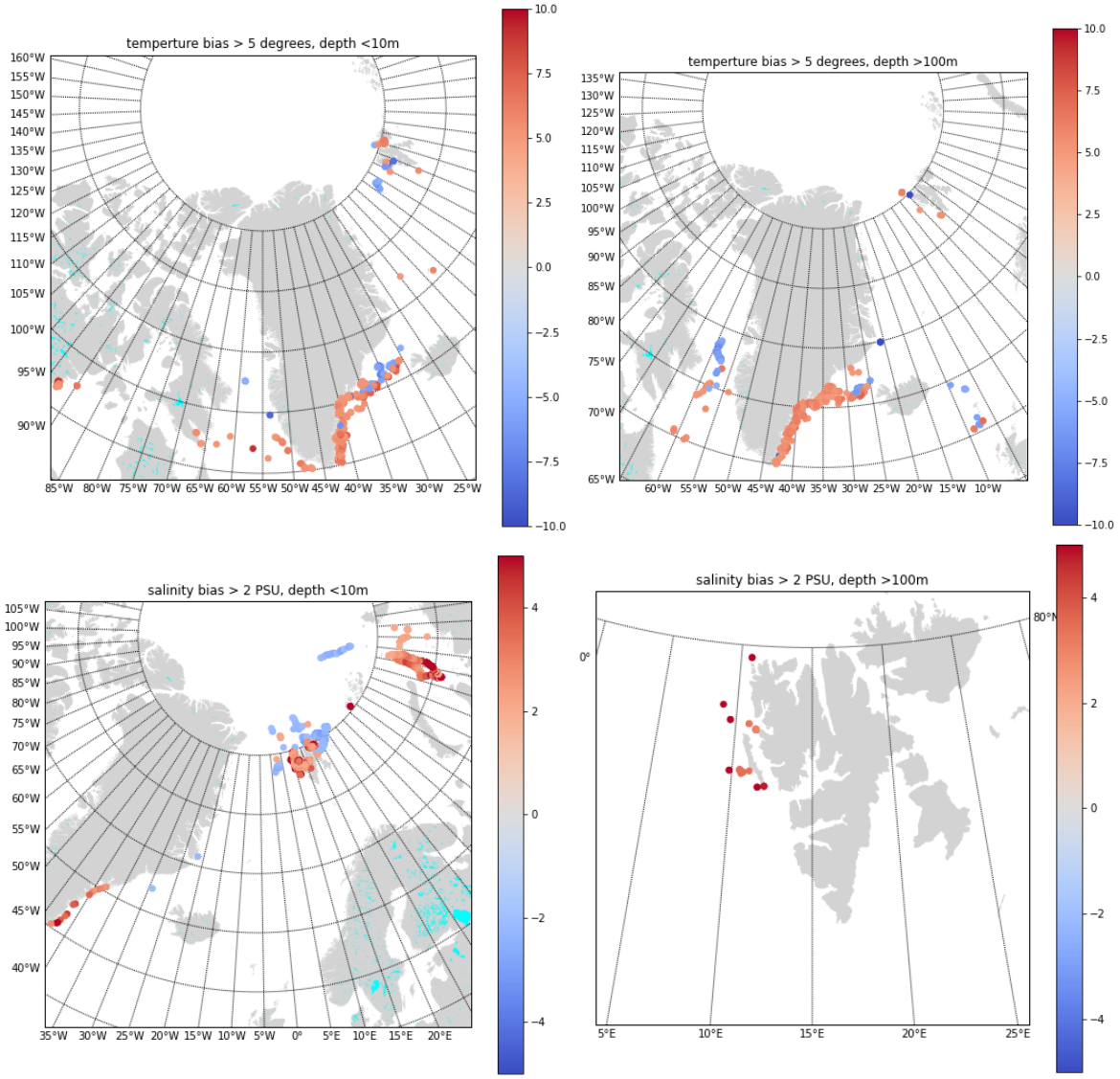

Figure 13. Stations with large model-observation differences: water temperature (upper panel), salinity (lower panel). For water temperature, large model bias was mainly found in the marginal ice zone (MIZ). In SE Greenland waters, the large bias was also found in lower layers. The model temperature is mostly higher than the observations. In the Greenland-Island Ridge MIZ, both warm and cold bias exists. For salinity in the upper 10m, the model has positive salinity bias in MIZ of SE Greenland and Svalbard. For deep layers, large positive bias only exists in coastal waters of Svalbard.

4.2.3 Specific analysis for the Greenland-Iceland-Faroe Island-Scotland Ridge region

The majority of the exchange between the Arctic Mediterranean and the North Atlantic occurs via passages between Greenland, Iceland, Faro Islands and the European continent, where an

underwater ridge system called the Greenland-Scotland Ridge (GSR) limits the exchanges. Warm saline water flows in the surface from the Atlantic into the Nordic Seas and further into the Arctic. Along its way this water is modified by atmospheric cooling and becomes denser, filling subsurface layers of the Arctic Ocean and the Nordic Seas. Dense water returns to the Atlantic through gaps in the GSR; these flows are known as "overflow" (Fig. 14).

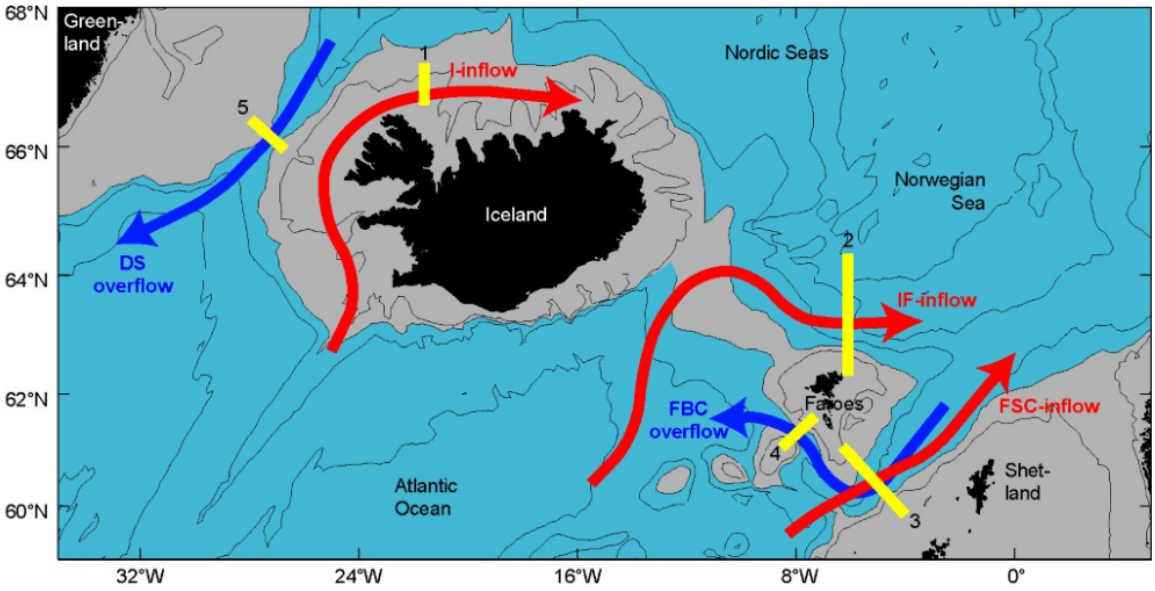

Figure 14. The GSR Transport Mooring Arrays (thick yellow lines marked with numbers) cover all three inflow branches (red arrows) and the two major overflow branches (blue arrows). 1: North Icelandic Irminger Current (NIIC; I-inflow), 2: Faroe Current (IF-inflow), 3: Faroe-Shetland Channel inflow (FSC-inflow), 4: Faroe Bank Channel overflow (FBC-overflow), 5: Denmark Strait overflow (DS-overflow) (Source: AtlantOS project).

In this section we look at details of model-observation intercomparison in the GSR region to document the value of marine mammal data for model validation.

For water temperature, the global model reanalysis is significantly warmer than the observations in the MIZ. One reason may be that melting sea ice requires energy, which is partly taken from the ocean and thereby locally lowers the temperature there. This mechanism may not be effectively represented or resolved in the model. Another reason may be that the model underpredicts the amount of ice in SE Greenland coastal-shelf waters thus resulting in a general warmer surface ocean (Fig. 15).

For salinity, there are much less salinity observations than for temperature due to the fact that only temperature sensor was available in the first a few years. In general, the reanalysis shows higher salinities than the observations. The largest salinity bias was in the MIZ in SE Greenland waters (Fig. 15).

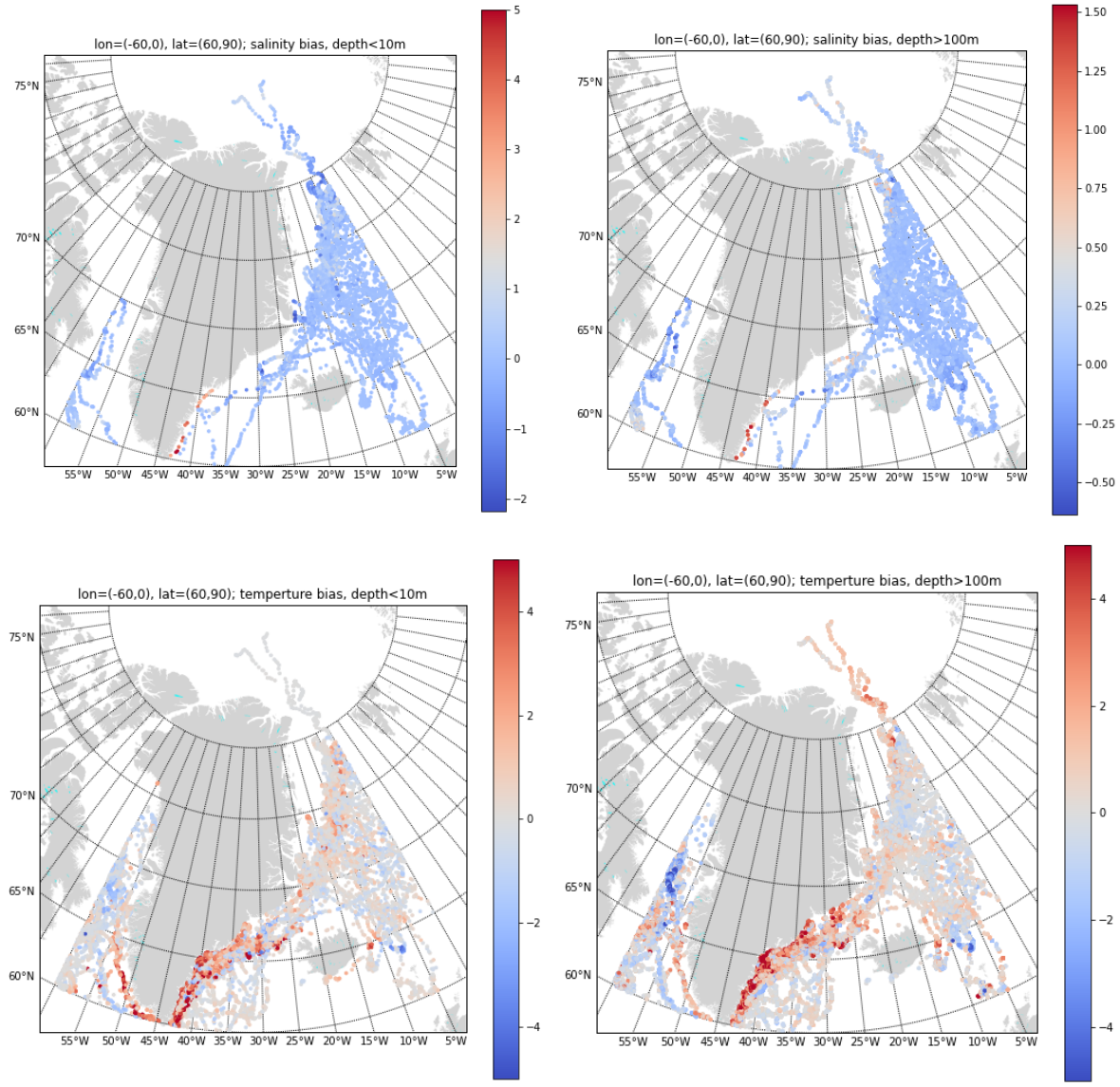

Figure 15. Differences between the observed and modelled water temperature and salinity in region (-60 – 0°E, 60 – 90°N). The results were made for different latitude-longitude sectors, temperature, salinity in the upper 10 m and also below 100 m.

5 Conclusions

Instruments mounted on fishing gear and on marine mammals are a cost-effective and emerging monitoring techniques in the Arctic Ocean Observing System. The used instruments are well tested and provides documented quality performance and are additionally calibrated before use, so the obtained observations are believed to live up to existing quality requirements to be used for model validation.

In this report fishing vessel and marine mammal T/S observations are compared with the ARC MFC analysis and 12 hour forecast data and CMEMS global reanalysis product, respectively. The observations used in this inter-comparison appear to be of high quality. The observations provide valuable information for model product validation, especially in coastal, MIZ and offshore waters. In general ARC MFC water temperature forecast is 0.3-1^{o}C colder than the observations. In the Baffin Bay, the inter-comparison of model-fishing gear data shows that the model has a shallower mixing layer in summer and sometimes a deeper mixed layer in the winter. In the coastal water, model surface salinity is generally to high compared to observations. In November 2019 the ARC MFC model ocean is found to be 1-2^{o}C warmer in 200-300 m depth in open waters around Faroe Islands. The observations in Norwegian coastal waters show that the model fails to simulate the 4-layer water mass vertical structure present in November 2020. These results may provide hints for further model improvements.

There are in total 682647 temperature observations and 452722 salinity observations available for the selected period. Salinity samples were not available until 2007. The average number of samples is 56887 for temperature and 37727 for salinity per month. The samples are evenly distributed in most of the months except for June and July where the amount of data only reach 35-60% and 21-42% of the monthly average for temperature and salinity, respectively. September has the largest amount of data which is 50% higher than the monthly average. Most data are collected in the Nordic Seas, Southeast Greenland, Davis Strait, Baffin Bay and Canadian Archipelago. Only a few percentages are from the Bering Sea. In the vertical dimension, the maximum sampling depth is about 1200 m. The amount of data decreases with depth. 80% of the temperature samplings and 85% of the salinity samplings are from the upper 100 m.

T/S observations measured by tagged sensors from marine mammals have been compared with CMEMS global daily reanalysis products. The results show that the global reanalysis has significant errors in MIZ regions, with temperature bias larger than 5 ^{o}C and surface salinity bias larger than 2 psu, which is much larger than observed in other ocean areas.

In the vertical direction, for water temperature, the model data bias and cRMSE are constant in the upper 50 m of about 0.18^{o}C and 1.16^{o}C, respectively. They increase with depth to reach the maximum values in 100-150 m depth (the depth of the thermocline) of 0.48^{o}C for bias and 1.57^{o}C for cRMSE. For salinity, the model ocean is saltier than the observations in all vertical layers, with the largest errors at the surface (0.50 psu for bias and 1.42 psu for cRMSE),

decreasing with depth and reaching a minimum in 600-700 m water depth (0.04psu for bias and 0.08psu for cRMSE).

Acknowledgement

The authors acknowledge constructive comments from Cooper Van Vranken at Berring Data Collective on the fishing gear observations.

References

Ali A., Christensen K.H, Breivik Ø, Malila M., Raj R.P., Bertino L., Chassignet E.P., Bakhoday-Paskyabi M. (2019) A comparison of Langmuir turbulence parameterizations and key wave effects in a numerical model of the North Atlantic and Arctic Oceans, Ocean Modelling, **137**, 76-97. https://doi.org/10.1016/j.ocemod.2019.02.005).

Bailleul, F., J. Vacquie-Garcia, and C. Guinet (2015). Dissolved oxygen sensor in animal-borne instruments: An innovation for monitoring the health of oceans and investigating the functioning of marine ecosystems. *PLoS ONE* 10(7):e0132681, https://doi.org/10.1371/journal.pone.0132681

Boehme, L., P. Lovell, M. Biuw, F. Roquet, J. Nicholson, S.E. Thorpe, M.P. Meredith, and M. Fedak (2009). Technical note: Animal-borne CTD-Satellite Relay Data Loggers for real-time oceanographic data collection.*Ocean Science* 5:685–695, https://doi.org/10.5194/os-5-685-2009.

Buch, E., M.S. Madsen, J. She, M. Stendel, O. K. Leth, A. M. Fjæraa and M. Rattenborg (2019). Arctic In-Situ Data Availability. https://insitu.copernicus.eu/library/reports/CopernicusArcticDataReportFinalVersion2.1.pdf

La Traon et al. (2019) From Observation to Information and Users: The Copernicus Marine Service Perspective. Front. Mar. Sci. 6, p234, https://www.frontiersin.org/article/10.3389/fmars.2019.00234 doi={10.3389/fmars.2019.00234},

Martinelli, M., Guicciardi, S., Penna, P., Belardinelli, A., Croci, C., Domenichetti, F., et al. (2016). Evaluation of the oceanographic measurement accuracy of different commercial sensors to be used on fishing gears. Ocean Eng. 111, 22–33. doi: 10.1016/J.OCEANENG.2015.10.037

Patti, B., Martinelli, M., Aronica, S., Belardinelli, A., Penna, P., Bonanno, A., et al. (2016). The fishery and oceanography observing system (FOOS): a tool for oceanography and fisheries science. J. Oper. Oceanogr. 9, s99-s118. doi: 10.1080/1755876X.2015.1120961

Photopoulou, T., M.A. Fedak, J. Matthiopoulos, B. McConnell, and P. Lovell (2015). The generalized data management and collection protocol for Conductivity-Temperature-Depth Satellite Relay Data Loggers. *Animal Biotelemetry* 3:21, https://doi.org/10.1186/s40317-015-0053-8.

Rignot, E.; Fenty, I.; Xu, Y.; Cai, C.; Velicogna, I.; Cofaigh, C.Ó.; Dowdeswell, J.A.; Weinrebe, W.; Catania, G.; Duncan, D. (2016). Bathymetry data reveal glaciers vulnerable to ice-ocean interaction in Uummannaq and Vaigat glacial fjords, west Greenland. Geophys. Res. Lett., 43, 2667–2674.

Roquet, F., J.B. Charrassin, S. Marchand, L. Boehme, M. Fedak, G. Reverdin, and C. Guinet (2011). Delayed-mode calibration of hydrographic data obtained from animal-borne satellite relay data loggers. Journal of Atmospheric and Oceanic Technology 28:787–801,https://doi.org/10.1175/2010JTECHO801.1.

Roquet, F., G. Williams, M.A. Hindell, R. Harcourt, C. McMahon, C. Guinet, J.-B. Charrassin, G. Reverdin, L. Boehme, P. Lovell, and others (2014). A Southern Indian Ocean database of hydrographic profiles obtained with instrumented elephant seals. *Nature Scientific Data* 1:140028, https://doi.org/10.1038/sdata.2014.28.

Treasure, A.M., F. Roquet, I.J. Ansorge, M.N. Bester, L. Boehme, H. Bornemann, J.-B. Charrassin, D. Chevallier, D.P. Costa, M.A. Fedak, C. Guinet, M.O. Hammill, R.G. Harcourt, M.A. Hindell, K.M. Kovacs, M.-A. Lea, P. Lovell, A.D. Lowther, C. Lydersen, T. McIntyre, C.R. McMahon, M.M.C. Muelbert, K. Nicholls, B. Picard, G. Reverdin, A.W. Trites, G.D. Williams, and P.J.N. de Bruyn (2017). Marine Mammals Exploring the Oceans Pole to Pole: A review of the MEOP consortium. Oceanography 30(2):132–138, https://doi.org/10.5670/oceanog.2017.234.

Van Vranken C, Vastenhoud BMJ, Manning JP, Plet-Hansen KS, Jakoboski J, Gorringe P and Martinelli M (2020). Fishing Gear as a Data Collection Platform: Opportunities to Fill Spatial and Temporal Gaps in Operational Sub-Surface Observation Networks. Front. Mar. Sci. 7:485512.doi: 10.3389/fmars.2020.485512